THE JOURNAL OF BIOLOGICAL CHEMISTRY VOL. 283, NO. 36, pp. 24729–24737, September 5, 2008

Lactaturia and Loss of Sodium-dependent Lactate Uptake in the Colon of SLC5A8-deficient Mice*

Received for publication, April 7, 2008, and in revised form, May 27, 2008 Published, JBC Papers in Press, June 17, 2008, DOI 10.1074/jbc.M802681200

Henning Frank[‡], Nicole Gröger[‡], Martin Diener[§], Christoph Becker[¶], Thomas Braun[‡], and Thomas Boettger[‡1]

From the [‡]Department of Cardiac Development and Remodelling, Max-Planck-Institut fuer Herz- und Lungenforschung, Parkstrasse 1, D-61231 Bad Nauheim, Germany, the [§]Institute for Veterinary Physiology, Justus-Liebig-University Giessen, D-35392 Giessen, Germany, and the [¶]Laboratory of Immunology, I. Medical Clinic, University of Mainz, 55131 Mainz, Germany

SLC5A8 is a member of the sodium/glucose cotransporter family. It has been proposed that SLC5A8 might act as an apical iodide transporter in the thyroid follicular cells or as a transporter of short chain monocarboxylates. We have directly addressed the functional role of SLC5A8 *in vivo* by generation of SLC5A8 mutant mice. We found that SLC5A8 is responsible for the re-absorption of lactate at the apical membrane of the kidney proximal tubules and of serous salivary gland ducts. In addition, SLC5A8 mediated the uptake of lactate into colonocytes under physiological conditions. We did not find any evidence of SLC5A8 being essential for the apical iodide transport in the thyroid gland, even if the ion-cotransporter SLC26A4, causing the human Pendred syndrome, is missing. Because SLC5A8 is transcriptionally silenced in many tumors, it has been proposed that SLC5A8-mediated transport of butyrate suppresses tumor formation. Treatment of *Slc5a8*$^{-/-}$ mice with carcinogens and breeding to the *Apc*^{min} mouse line did not reveal a higher incidence of tumor formation. We conclude that SLC5A8 is instrumental in preventing lactaturia and loss of sodium-dependent uptake of lactate in the colon but does not have any apparent role in the prevention of tumor formation and growth.

Slc5a8 belongs to the sodium/glucose cotransporter family *Slc5*. Loss of function of these transporters may cause intestinal glucose/galactose re-absorption defects, glucosurea, or in the case of the Na^+/I^- symporter (NIS,[2] *SLC5A5*) hypothyroidism in humans (1). *NIS* is expressed in the basolateral membrane of thyroid follicular cells and mediates the uptake of iodide from blood into the cytoplasm of thyrocytes. Iodide is transported across the cytoplasm to the apical membrane toward the follicle lumen where it is oxidized and bound to thyroglobulin. A candidate molecule to mediate the efflux of iodide at the apical membrane is SLC26A4, which is mutated in Pendred syndrome, a genetic disorder that is associated with profound sensorineural hearing loss and goiter (2, 3). It has been shown *in vitro* in a polarized cell system that SLC26A4 can mediate the efflux of iodide via the apical membrane of a cell (4). Nevertheless, a knockout mouse model for *Slc26a4* does not show any signs of thyroid dysfunction, challenging the role of *Pendrin* in iodide transport at the apical membrane of thyrocytes (5). SLC5A8 was first described as a close structural relative of human NIS (46% identity and 70% similarity), but in contrast to NIS, it is expressed at the apical membrane of thyrocytes (6). The expression of SLC5A8 reduces iodide accumulation in NIS-transfected COS-7 cells, compatible with a role of SLC5A8 as a transporter that may mediate the flux of iodide ions into the follicular lumen of the thyroid (6). Thus, SLC5A8 was designated human **A**pical **I**odide **T**ransporter (hAIT). Later it was shown that SLC5A8 overexpressed in *Xenopus laevis* oocytes mediates the sodium-coupled transport of monocarboxylates like L-lactate, propionate, butyrate, or nicotinate, whereas exposure to iodide or bromate did not lead to currents (7–9). The sodium-dependent transport of monocarboxylates by SLC5A8 was also corroborated in a mammalian expression system (10) leading to renaming of the molecule as **S**odium **M**ono**c**arboxylate **T**ransporter 1 (SMCT 1).

Because of glomerular filtration of lactate from blood to primary urine, lactate needs to be re-absorbed efficiently in the kidney to prevent lactaturia. Several studies suggest a sodium-dependent lactate re-absorption in the brush border membrane of the renal proximal tubule (11). SLC5A8 has been considered to be instrumental in lactate re-absorption in the S3 segment of the renal proximal tubule (10, 12) together with the related transporter SLC5A12 (SMCT2) in the S1 and S2 segment of the proximal tubule (12–14). However, clear evidence for the role of SLC5A8 in lactate re-absorption in the kidney is still lacking.

In addition to its physiological function in homeostasis of short monocarboxylates, a number of reports suggested a role for SLC5A8 in carcinogenesis. Because exon 1 of the *SLC5A8* gene is aberrantly methylated in 59% of primary human colon cancers and in 52% of the analyzed colon cancer cell lines, it was proposed that *SLC5A8* might act as a tumor suppressor gene (15). Similarly, re-expression of SLC5A8 in colon cancer cell lines lacking SLC5A8 suppressed colony growth (15). Potential tumor suppressive effects of SLC5A8 were also demonstrated for colon cancer (9), gastric cancer (16), thyroid cancer (17), and oligodendroglioma (18). It was claimed that SLC5A8-mediated transport of butyrate might serve as the molecular basis for the tumor suppressive role of *SLC5A8* (19).

Here we demonstrate that SLC5A8 is expressed in the apical membranes of cells in the kidney, intestine, thyroid, and sali-

* This work was supported in part by a grant from the Deutsche Forschungsgemeinschaft (to T. B.), by the Max-Planck Society, and by the Excellence Cluster Cardiopulmonary System. The costs of publication of this article were defrayed in part by the payment of page charges. This article must therefore be hereby marked "*advertisement*" in accordance with 18 U.S.C. Section 1734 solely to indicate this fact.

[1] To whom correspondence should be addressed: Dept. of Cardiac Development and Remodelling, MPI fuer Herz- und Lungenforschung, Parkstrasse 1, D-61231 Bad Nauheim, Germany. Tel.: 49-6032-705-203; Fax: 49-6032-705-211; E-mail: thomas.boettger@mpi-bn.mpg.de.

[2] The abbreviations used are: NIS, Na^+/I^- symporter; WT, wild type; KO, knock-out; SMCT, sodium monocarboxylate transporter; TSH, thyroid-stimulating hormone; TRITC, tetramethylrhodamine isothiocyanate.

vary gland, but not in the brain, as defined by RNA *in situ* hybridization and a newly derived antibody directed against the C terminus of the protein. The generation of a loss of function mouse model of *Slc5a8* revealed that SLC5A8 is essential for lactate re-absorption in the kidney and for adjusting lactate concentration in saliva. But it is dispensable for iodide transport in the thyroid gland even in the absence of the ion-cotransporter SLC26A4 responsible for the human Pendred syndrome. In the colon, we detected a sodium-dependent current induced by an addition of lactate to the luminal side that was mediated by SLC5A8, while no evidence was found for a SLC5A8-dependent butyrate transport in the colon. Our study reveals that SLC5A8 has no apparent role in the prevention of tumor formation and growth in the colon.

EXPERIMENTAL PROCEDURES

Targeting Construct and Mutant Mice—The mouse genomic clone was derived from a 129/ola cosmid library. A loxP-flanked neomycin-resistance cassette was inserted into a BamHI site in front of the fourth exon. A loxP site was inserted into the HpaI site following the fifth exon of *Slc5a8* (NP_145423.2). The resulting targeting vector contained 10.9 kb of 5′- and 6.1 kb of 3′-flanking sequence (Fig. 1*A*). Mouse embryonic stem cells were electroporated, and mouse lines recombinant for the *Slc5a8* locus were established from two independent ES clones. Heterozygous animals of each clone were mated to Meu-Cre40 mice (20) to remove the neo^R-cassette and 2.7 kb genomic sequence. The loss of exons 4 and 5 results in a frameshift and truncation of the SLC5A8 protein after 4 of at least 10 transmembrane domains. The study was performed in a mixed 129SV/C57Bl6 background. ES cells and mice were genotyped using a BamHI digest and a 3′ probe (Fig. 1*H*). The Apc^{Min} strain is commercially available from Jackson Laboratory. The *Slc26a4* knock-out mice were provided as cryoconserved embryos by Eric Green (5).

In Situ Hybridization, Immunofluorescence, and Western Blot—For *in situ* hybridization, 12-μm cryosections were prepared. The templates for probe transcription were 1175 bp of Slc5a8 cDNA (5′ cgtacacatgatgcttcagttttgg, 3′ catgaaacaaaccacatgacgtgtg) and of 994 bp of Slc5a12 cDNA (5′ tgtactttaacttgttgggtctctgg, 3′ gggttgtagcctggaatctgagccaa) amplified by RT-PCR. A polyclonal antiserum was raised against a peptide sequence (VFKKRNHVLNYKLHPVEVGC) close to the SLC5A8 C terminus. The serum was affinity-purified against the peptide sequence. Other primary antibodies were α-MCT 1 (1:300; Chemicon), α-laminin (1:100; DSHB), α-fibronectin (1:100; BD Biosciences); Secondary antibodies (1:2000) were Alexa Fluor 488 goat α-mouse, Alexa Fluor 546 goat α-rabbit, Alexa Fluor 488 goat α-rabbit (Invitrogen), or sheep α-rabbit IgG-HRP (Chemicon, 1:5000). TOTO-3 or DAPI (both 1:1000; Invitrogen) were used for nuclear staining, Phalloidin-TRITC (1:1000, Sigma) for actin labeling. For immunofluorescence, appropriate tissues of $Slc5a8^{-/-}$ mice were used as controls. Protein extracts from tissues were prepared by homogenization in 3 ml of buffer (125 mM NaCl, 20 mM Tris/HCl, pH 8.0, 4.5 mM EDTA, Complete protease inhibitor mixture (Roche 11836153001). Extracts were centrifuged at 1000 × *g* for 10 min. From the supernatant, proteins were collected at 135,000 × *g* for 1 h. The pellet was resuspended in 100 μl of sample buffer (100 mM Tris/HCl, pH 8.0, 10 mM EDTA, 40 mM dithiothreitol, 10% SDS, Complete protease inhibitor mixture). The protein concentration was determined using the DC Protein Assay kit (Bio-Rad 500-0111). 10 μg of protein extracts (0.3 μg for kidney) were separated on 4–12% SDS-PAGE gradient gels and transferred onto nitrocellulose membranes (Invitrogen). By using horseradish peroxidase-coupled secondary antibody and SuperSignal Femto detection solution (Perbio Science), signals were detected with a VersaDoc Imaging System (Bio-Rad).

Metabolic Cages—Single mice were kept in mouse metabolic cages (Techniplast) with free access to water and chow. After adaptation to the cage, urine and feces were collected over 24-h periods. The analysis of urinary electrolytes was performed by Vet Med Lab (Ludwigsburg, Germany).

Measurement of Lactate in Blood and Saliva—Blood for analysis of lactate concentration was collected from the tail tip. For saliva collection, animals were fasted for 5 h before the experiment. To activate salivation, mice were injected with 5 mg of pilocarpine per kg of bodyweight. After 2 and 4 min, saliva was collected from the mouth of the animals. The lactate concentration was determined by Lactate Scout (SensLab, Germany).

Histology—Tissue samples (large intestine, kidney, submandibular gland, and thyroid) were perfused and fixed with 4% paraformaldehyde, dehydrated, and embedded in paraffin. Samples were stained with hematoxylin and eosin and examined for histological changes by light microscopy.

Carcinogen Treatment—Treatments were performed with 5-month-old mice. A single lot of azoxymethane (AOM) was used (Sigma-Aldrich, 100-mg isovials). Each 100-mg vial was resuspended in 3.9 ml of phosphate-buffered saline and aliquots were stored at −20 °C. A 1 μg/μl working solution was prepared in 0.9% NaCl. Mice were treated intraperitoneally with 10 mg of AOM per kg of body weight once a week for 8 weeks (21, 22). Second, 2% sodium dextran sulfate (MW: 36,000–50,000, MP Biomedicals, Inc.) was added to the drinking water for 1 week, followed by a 2-week-period with drinking water. This treatment was repeated three times (23). Three months after the end of the respective treatment, tumor development was scored by endoscopic examination as previously described (24). In brief, all visible tumors were counted and graded by the following criteria: grade 1-very small but detectable; grades 2–5: tumor covering up to one-eighth [2], up to one-fourth [3] up to one-half [4], more than one-half [5] of the colonic circumference.

RNA Expression Analysis—Total RNA from colon was isolated with the TRIzol (Invitrogen) method. RNA concentrations were measured using a NanoDrop ND-1000 spectrophotometer (NanoDrop Technologies). RNA quality was confirmed using RNA 6000 Nano LabChip kit (Agilent 2100 Bioanalyzer). RNA integrity numbers for the 10 samples ranged from 8.9 to 9.6. For Affymetrix GeneChip Mouse Genome 430 2.0 hybridization, 10 μg of total RNA were used for sample preparations as suggested by the Affymetrix Eukaryotic Target Protocol. Affymetrix Quality Control Reporter tool was used to assure the uniform performance of the individual GeneChip hybridizations with present calls between 52 and 56% for all

GeneChips and comparable 3′/5′ ratios for the internal controls. Data were analyzed using Stratagene Arrayassist 5.5.1. For background correction, normalization, and probe summarization we used the RMA algorithm (25). To suppress noise at very low signal intensities, variance stabilization was performed. Data were log-transformed to base 2 and baseline transformed with the WT group as baseline. An asymptotic *t* test was performed. To account for multiple hypothesis testing, Benjamini-Hochberg (26) and alternatively Westfall-Young (27) correction were performed. For real-time RT-PCR we used an iCycler iQ^{TM} (Bio-Rad) using the Absolute QPCR SYBR Green Fluorescein mix (Abgene). Values were normalized to an endogenous reference: SQ_{target}/SQ_{HPRT}.

Analysis of Thyroid Function—The T4 concentration was measured by using a commercial RIA (Diagnostic Systems Laboratories, Inc., Beckmann Coulter). As an internal control, we used serum from mice fed with iodide-depleted nutrition (Altromin) containing 0.15% propylthiouracil (PTU, Sigma) for 10 days. TSH measurement was performed by Dr. Parlow (National Hormone & Peptide Program; Harbor-UCLA). The efficiency of iodide incorporation into thyroglobulin was measured as described (28). Briefly, we injected 15 μCi of $^{125}I^-$ (Amersham Biosciences) intraperitoneally. After 1 h, animals were anesthetized; thereafter blood was taken from the heart with a syringe and the thyroid was excised. To block unspecific binding of ^{125}I to hemoglobin, iodide to a final concentration of 6 mM was added to the blood sample (29). Unbound $^{125}I^-$ was removed from serum by Zebra^{TM} Desalt Spin Columns (Pierce). The ratio protein-bound ^{125}I/free serum $^{125}I^-$ over time is a measure of thyroid function. A second readout for $^{125}I^-$ organification was the ratio protein-bound ^{125}I in serum/$^{125}I^-$ taken up into the thyroid over a 1-h period. To evaluate the method, a time course series of the iodide incorporation was performed. A 1-h period was chosen between $^{125}I^-$ injection and blood sampling.

Ussing Chamber Analysis—A 3-cm long proxomedial part of the colon was removed, and the colonic lumen was rinsed with ice-cold Parsons solution. This standard buffer for the Ussing chamber experiments contained (mM): 107 NaCl, 4.5 KCl, 25 $NaHCO_3$, 1,8 Na_2HPO_4, 0.2 NaH_2PO_4, 1.25 $CaCl_2$, 1 $MgSO_4$, and 12 glucose. The solution was gassed with carbogen; pH was 7.4. The addition of lactate did not change this pH. For the Na^+-free solution, NaCl was replaced by *N*-methyl-D-glucamine ($NMDG^+$) chloride. The tissue was fixed in a modified Ussing chamber, bathed with a volume of 3.5 ml on each side of the mucosa, and short-circuited by a computer-controlled voltage-clamp device (Mu*β*ler Ingenieurbüro, Aachen, FRG) with a correction for solution resistance. The exposed surface of the tissue was 1 cm^2. Short-circuit current (I_{sc}) was continuously recorded, and tissue conductance (Gt) was measured every min by applying a current pulse of $\pm$ 50 $\mu A \cdot cm^{-2}$. I_{sc} is expressed as $\mu Eq \cdot h^{-1} \cdot cm^{-2}$, *i.e.* the flux of a monovalent ion per time and area, with 1 $\mu Eq \cdot h^{-1} \cdot cm^{-2}$ = 26.9 $\mu A \cdot cm^{-2}$. For statistical analysis, we calculated the ratio between the maximal decrease of the I_{sc} within 5 min after lactate addition and the mean I_{sc} 3 min before lactate addition. To determine the unidirectional mucosa-to-serosa flux (J_{ms}) of butyrate, sodium [^{14}C]butyrate (37 kBq, Hartmann Analytical, Braunschweig, Germany) was added to the mucosal side after an equilibration period of 30 min. For these experiments, the mucosal buffer contained 5 mM sodium butyrate and the serosal buffer contained 8 mM mannitol for osmotic compensation. After an additional 30 min to allow isotope fluxes to reach a steady state, unidirectional ion fluxes were determined over two sequential 20-min periods. Both periods were averaged to calculate the flux rate. All aliquots from the labeled side were replaced by unlabeled buffer solution, and an appropriate correction for this replacement solution was performed. The radioactivity in the samples was determined in a liquid scintillation counter (TRIS-CARB® 2700 TR Liquid scintillation analyser, Packard, Frankfurt, Germany). The unidirectional mucosa-to-serosa flux (J_{ms}) is indicated as transported amount of butyrate per surface area and time [$\mu mol \cdot cm^{-2} \cdot h^{-1}$].

Statistics—An unpaired Student's *t* test assuming equal variances or a Mann-Whitney test was used to compare data from two treatment groups.

RESULTS

Homozygous Mutant SLC5A8 Mice Are Viable and Fertile and Lack Major Morphological Malformations—The *Slc5a8* locus was modified in ES cells by targeted recombination resulting in the integration of a neomycin-resistance cassette flanked by loxP sites upstream of the fourth exon and an additional loxP site downstream of the fifth exon (Fig. 1*A*). Mice homozygous for the integrated targeting vector did not show any obvious phenotype. To delete the selection cassette and generate a null allele of *Slc5a8*, mutant mice were bred to Meu-Cre40 mice resulting in the deletion of a 2.7-kb fragment encompassing the fourth and fifth exon (Fig. 1*A*). Heterozygous progeny, which were Cre-recombinase negative were backcrossed to C57BL6 mice and mated to each other to generate homozygous mutant animals. Homozygous animals were viable and fertile and did not show any obvious phenotype regarding weight, morphology, or motility.

SLC5A8 Is Expressed in Apical Membranes of Different Epithelial Cells—RNA *in situ* hybridizations were performed on different organs and sagittal sections of mice 1 day after birth with a specific probe for *Slc5a8*. We observed a strong expression of *Slc5a8* in the submandibular gland, kidney, and gut at P1 (Fig. 1, *B–D*). In the adult kidney, we detected *Slc5a8* mRNA in the kidney cortex, with more intense signals in the inner cortex (Fig. 1*E*). The related Na^+-monocarboxylate transporter *Slc5a12* was mainly detected in the outer cortex of the kidney (Fig. 1*F*) as previously described (13).

SLC5A8 expression was also investigated by Western blot analysis of multiple organs with an affinity-purified antiserum against a peptide close to the C terminus of the protein. Specific signals were detected in kidney, salivary gland, and large intestine (Fig. 1*I*). We did not detect the protein in brain and heart (Fig. 1*I*), liver, lung, spleen, muscle, testis, and uterus (data not shown). Immunofluorescence staining using the affinity-purified antiserum revealed a strong expression in the kidney, intestine, thyroid, and salivary gland, but not in the brain. The domains of protein expression corresponded well with expression of the mRNA detected by *in situ* hybridization. The expression of SLC5A8 in the kidney was confined to the cortex and the

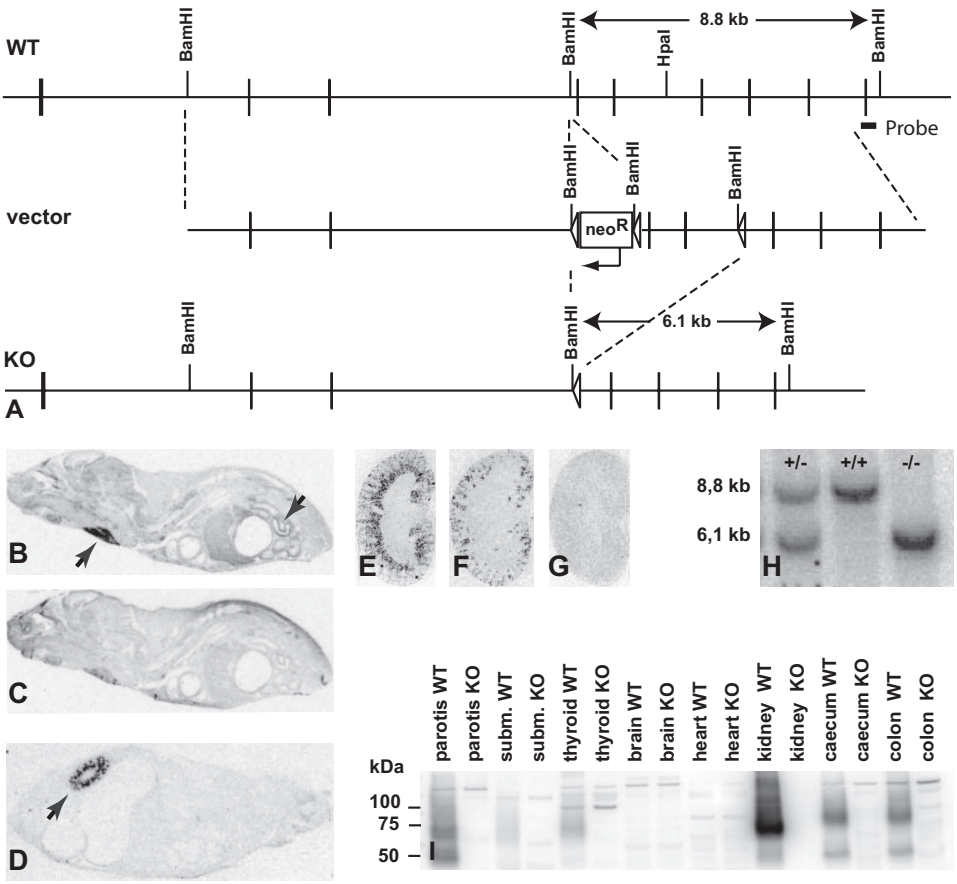

FIGURE 1. **Targeting of the *Slc5a8* gene, RNA *in situ* hybridization, Southern, and Western blot analysis.** *A*, targeting vector was prepared with loxP sites flanking the 4th and 5th coding exons of *Slc5a8* and a neomycin resistance cassette that was inserted upstream of the 4th exon. ES cells with identified homologous recombination were used to generate chimeras by blastocyst injection. Germline heterozygous animals were bred to Meu-Cre40 mice to delete the 4th and 5th exon of the *Slc5a8* locus as well as the neomycin resistance cassette. RNA *in situ* hybridization. *B–G*, sagittal sections of a P1 mouse (*B–D*) hybridized with a *Slc5a8*-specific antisense (*B* and *D*) or a sense (*C*) riboprobe. Expression was observed in the submandibular gland, in the gut (*B*, *arrows*), and in the kidney (*D*, *arrow*). Sagittal sections of adult kidneys (*E–G*) were hybridized with a *Slc5a8* (*E*), a *Slc5a12* antisense (*F*), or a sense probe (*G*). Southern blot of transgenic animals using the 3′ outside probe: 8.8 kb indicates the WT, 6.1 kb indicates the KO allele (*H*). The Western blot specifically detects SLC5A8 in kidney, salivary gland, thyroid, caecum, and colon. (*I*).

outer stripe of the outer medulla (Fig. 2*A*). The presence of SLC5A8 was restricted to the brush border of proximal tubules as indicated by costaining with phalloidin-TRITC, which identifies the brush border of the proximal tubules. Almost all proximal tubules of the outer stripe of the outer medulla were labeled, whereas many proximal tubules of the outer kidney cortex are devoid of SLC5A8 protein. Similar observations were also made by Gopal *et al.* (10) who described the expression of SLC5A8 in the S3 segment of the proximal tubule. The expression of SLC5A8 in the thyroid gland was limited to the apical membrane of follicular cells (Fig. 2*B*). In the parotid gland, we detected expression of SLC5A8 at the apical membranes of intercalated duct cells (Fig. 2*C*) and of the acini (not shown). In the submandibular gland, immunoreactivity was only found in the apical membrane of the serous acini while the mucosal acini of this mixed salivary gland were negative for SLC5A8 (Fig. 2*D*). In the digestive tract, a double staining of monocarboxylic acid transporter 1 (MCT1, SLC16A1) and SLC5A8 was carried out. SLC5A8 was present in the apical membrane of both the surface epithelium and in crypts, whereas MCT1 labeling was exclusively observed in the basolateral membrane of surface epithelium and crypts. The intensity of SLC5A8 staining increased from the small intestine to the colon (Fig. 2, *E–I*). The jejunum presented a very faint but specific apical signal (not shown), whereas no immunoreactivity for SLC5A8 was detected in the duodenum and stomach (not shown). The anti-MCT1 (SLC16A1) antibody intensely labeled the large intestine (Fig. 2, *F–J*) but not the small intestine (Fig. 2*E*). The specificity of signals was always confirmed by parallel processing of the respective *Slc5a8*$^{-/-}$ tissues (Fig. 3*K*).

SLC5A8 and SLC26A4 Alone and in Combination Are Dispensable for Normal Function of the Thyroid Gland—To investigate a possible role for SLC5A8 in the transport of iodide in the thyroid gland we measured the function of the thyroid in *Slc5a8*$^{-/-}$ and in *Slc5a8*$^{-/-}$/*Slc26a4*$^{-/-}$ compound mutant mice. Histological investigation of the thyroid of up to 2-year-old *Slc5a8*$^{-/-}$ animals did not reveal any changes in the size of the thyroid or any other obvious morphological abnormalities. The histological examination was repeated in 5-month-old animals from *Slc5a8*/*Slc26a4* cross-breedings. As expected, we did not observe any changes in morphology of *Slc5a8*$^{-/-}$ or *Slc26a4*$^{-/-}$ thyroids (Fig. 3, *A–C*); neither did we observe any apparent pathological changes in the thyroidea of *Slc5a8*/*Slc26a4* compound mutant mice (Fig. 3*D*). We also analyzed the concentration of T4 in all different genotypes; no significant differences of T4 concentrations were detected (WT/WT: 2.27 ± 0.33 μg/dl (n = 6); *Slc26a4*$^{+/+}$/*Slc5a8*$^{-/-}$: 2.56 ± 0.37 (n = 8); *Slc26a4*$^{-/-}$/*Slc5a8*$^{+/+}$: 2.06 ± 0.27 (n = 8); KO/KO: 2.8 ± 0.33 (n = 8)). The concentration of TSH in blood was determined for WT (160 ± 7.0) and *Slc5a8*$^{-/-}$ (166 ± 7.2 ng/ml serum; n = 25/23) and was not significantly different. For WT *versus* *Slc5a8*$^{-/-}$ we also measured the $^{125}I^-$ incorporation into the serum protein as a measure for thyroid iodide organification as the percentage bound ^{125}I/unbound $^{125}I^-$ in serum after 1 h of incorporation. We did not detect any difference in WT (0.68% ± 0.17%) *versus* Slc5a8$^{-/-}$ (0.70% ± 0.17%); (n = 6). Second, we calculated the percentage of protein-bound ^{125}I per ml of serum per $^{125}I^-$ in the thyroid after 1 h. Again, we did not detect any difference between WT (1.2% ± 0.4%; n = 6) and *Slc5a8*$^{-/-}$ (1.4% ± 0.5%; n = 6; p = 0.378), indicating that SLC5A8 is dispensable for normal function of the thyroid gland.

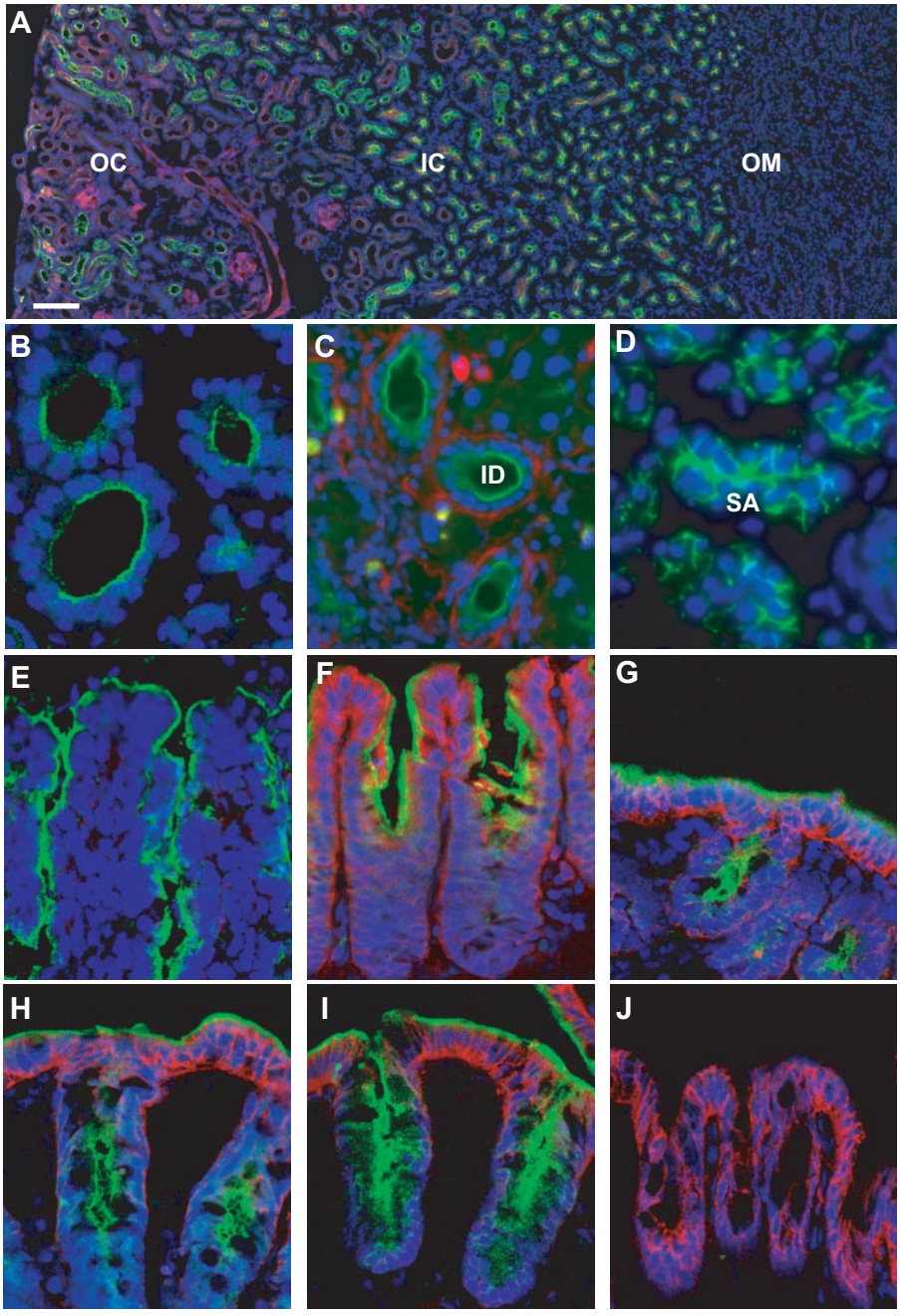

FIGURE 2. **Immunofluorescence localization of SLC5A8 in the kidney, thyroid gland, submandibular gland, parotid gland, and intestine.** The SLC5A8 specific antiserum (*green*) and nuclear labeling (*blue*) DAPI or TOTO-3 was used. *A*, expression of SLC5A8 in outer (*OC*) and inner kidney cortex (*IC*) as well as in the outer stripe of the outer medulla (*OM*), co-stained for actin with phalloidin (*red*). *B*, staining of SLC5A8 at the apical membrane of thyroid follicular cells. *C*, SLC5A8 expression of the apical membrane of the intercalated duct (*ID*) cells of the parotis, co-stained with α-fibronectin antibody (*red*). *D*, apical localization of SLC5A8 in the serous acini (*SA*) of the submandibular gland identified by their specific morphology. Apical expression of SLC5A8 was observed in ileum (*E*), caecum (*F*), proximal colon (*G*), medial colon (*H*), and distal colon (*I*). The respective *Slc5a8*$^{-/-}$ tissues were used as negative controls. In *J*, the colon of a *Slc5a8*$^{-/-}$ animal is shown. *E–J*, the basolateral membrane was labeled with an antibody against MCT1 (*red*). The *scale bar* in *A* corresponds to 100 μm in *A* and 18 μm in *B–J*.

Slc5a8$^{-/-}$ *Mice Are Unable to Re-absorb Lactate from Urine and Saliva*—Daily water and food uptake of WT and *Slc5a8*$^{-/-}$ mice (n = 24) and 24 h of urine release were measured using metabolic cages. Analysis of the electrolyte composition of the urine revealed a massive increase of the urinary lactate concentrations (>67-fold, Fig. 4*A*). Interestingly, the concentration of Na^+, K^+, Mg^{2+}, Ca^{2+}, Cl^-, inorganic phosphate, creatinine, glucose, urea, and uric acid in the urine was not significantly changed. Because no morphological alterations were apparent in the kidney, even in H&E-stained sections of >2-year-old animals, we conclude that the lactaturia did not impair other functions of the kidney or caused morphological malformations (not shown). SLC5A8 being strongly expressed in the salivary gland, we examined the salivary lactate concentration in KO *versus* WT animals after intraperitoneal injection of pilocarpine to stimulate salivation. The saliva was collected 2 and 4 min after injection, and lactate concentrations were measured. KO mice showed a significant increase of salivary lactate concentration both after 2 min (Fig. 4*B*) and 4 min after pilocarpine injection (not shown). The concentration of lactate in the blood was not changed (WT: 2.05 ± 0.11 mM; KO: 2.20 ± 0.12 mM; n = 20/30) indicating that *Slc5a8*$^{-/-}$ mice efficiently compensated for the loss of lactate.

The Absence of SLC5A8 Does Not Increase Susceptibility to Colon Cancer—SLC5A8 silencing by methylation has been previously described to support tumor formation and growth in the colon and elsewhere (7–9, 15, 16, 19, 30–32). Hence, we examined the large intestine of *Slc5a8*$^{-/-}$ and WT mice older than 20 months for the formation of tumors using histological techniques and colonoscopy (24). No spontaneously developed tumors were found in these animals (n = 13/13). We did not observe any signs of inflammation in WT or *Slc5a8*$^{-/-}$ nor did we detect an increased fecal ammonia excretion (data not shown). To get a more detailed insight into the physiological process that might be affected by the loss of *Slc5a8*, we analyzed transcriptional profiles of WT and *Slc5a8*$^{-/-}$ colon using Affymetrix GeneChips (n = 5/5). Statistical analysis of the data using the asymptotic t test results in a number of genes with low p values that is always below the number of genes that one expects for that p value according to multiple hypothesis testing. After Benjamini-Hochberg (26) or Westfall-Young (27)

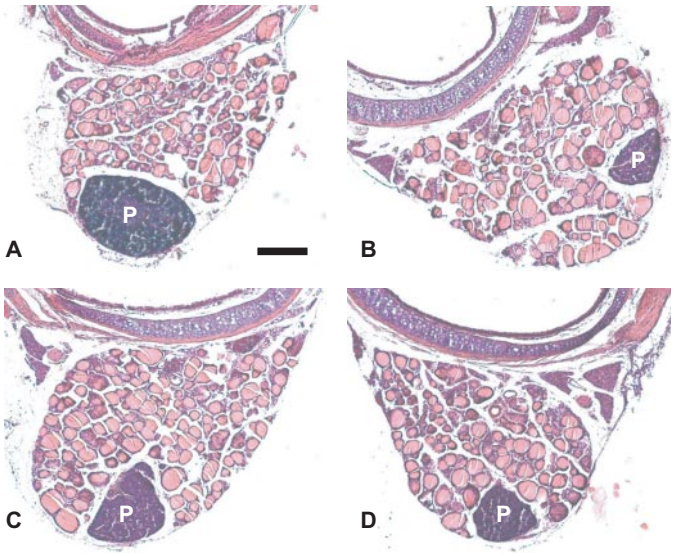

FIGURE 3. **Histological sections of the thyroid of *Slc5a8*$^{-/-}$/*Slc26a4*$^{-/-}$ mice.** Sections (12 μm) are stained with hematoxylin/eosin. *A*, WT; *B*, *Slc5a8*$^{-/-}$; *C*, *Slc26a4*$^{-/-}$; *D*, *Slc5a8*$^{-/-}$/*Slc26a4*$^{-/-}$. No differences in thyroid histology between the four genotypes were observed. *P*, parathyroid gland. The *scale bar* corresponds to 200 μm.

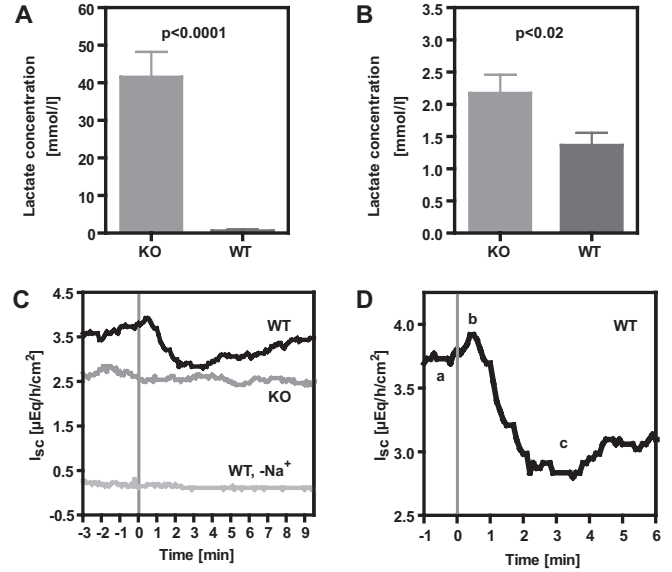

FIGURE 4. **Urinary and salivary lactate excretion of WT and *Slc5a8*$^{-/-}$ mice.** *A*, urinary lactate concentration (n = 23/group). *B*, salivary lactate concentration after 2 min after pilocarpine injection (n = 13/group). *C* and *D*, lactate transport in the proxomedial colon as recorded by the Ussing chamber assay. Typical recordings are shown in *C*: L-lactate (2 mM) was added to the luminal side of the WT or *Slc5a8*$^{-/-}$ colon at t = 0, sodium-free medium abolishes the lactate-stimulated currents in WT. *D*, magnification of the WT curve, to illustrate the initial rise of the short circuit current (*ab*), followed by a strong diminishment (*bc*) most probably because of swelling-activated basolateral Cl^- channels. Statistical analysis of the diminishment of the I_{sc} proves the significance of the difference WT *versus* *Slc5a8*$^{-/-}$ (n = 6/6; $p < 0.025$) and WT *versus* WT Na^+-free medium (n = 6/5; $p < 0.001$).

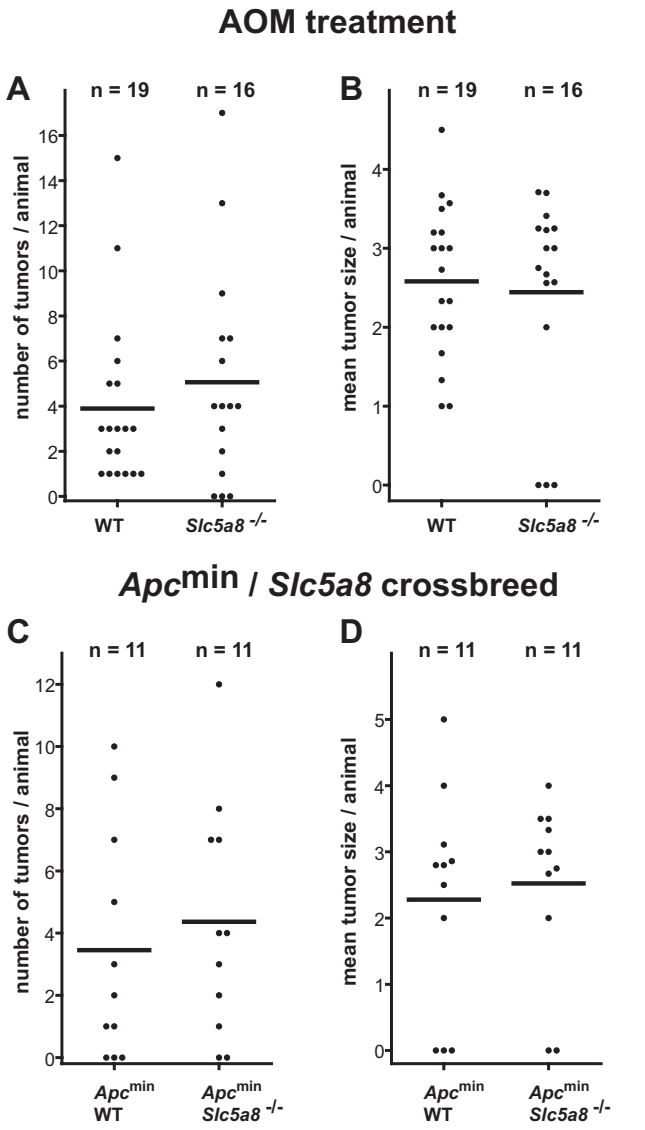

FIGURE 5. **Tumor number and size after carcinogen treatment and cross-breed of *Slc5a8* with *Apc*^{min}.** Scatter blots with mean are shown. The Mann-Whiney test was used for statistical analysis. *A* and *B*, tumor induction in WT and *Slc5a8*$^{-/-}$ mice treated with azoxymethane. There is no difference in the number of induced tumors ($p > 0.45$) nor the tumor size ($p > 0.75$). *C* and *D*, tumor development in WT and *Slc5a8*$^{-/-}$ after cross-breeding to a heterozygous *APC*^{min} allele. Neither tumor number ($p > 0.55$) nor tumor size ($p > 0.55$) is significantly changed.

correction, the only significantly changed probeset was 1425606_at detecting the *Slc5a8* 3′-untranslated region, whose sequence is not affected by the deletion of exons 4 and 5 in *Slc5a8*$^{-/-}$. Signal intensities for the *Slc5a8* transcript were low in *Slc5a8*$^{-/-}$ (293 ± 42) compared with WT (2193 ± 195). The acetylation status of histones in colonocytes is considered to be affected by the monocarboxylate transport of SLC5A8, leading to transcriptional changes (16, 19, 32). We did not find any evidence for this hypothesis. The regular gene expression profile in colonocytes as obtained by Affymetrix GeneChip analysis clearly suggested that loss of SLC5A8 expression does not have a significant gene regulatory effect (n = 5/5; data not shown). To confirm this conclusion, we also examined the expression of p53 in *Slc5a8* mutant mice by real time RT-PCR (n = 6/6). Again, there were no significant differences between WT and mutant mice.

Because the absence of an increased tumor incidence in *Slc5a8* mutant mice at physiological conditions does not rule out loss of SLC5A8 increasing the susceptibility of tumor formation, we tested the effects of different tumor induction models using different carcinogen treatments in 5-month-old WT and *Slc5a8*$^{-/-}$ mice (Fig. 5). First, mice were treated intraperi-

toneally with azoxymethane (21) once a week for 8 weeks (21). Three months after the last injection, mice were studied by colonoscopy, and tumor development was scored (24). Almost all animals of this group developed tumors, although no significant differences between WT and *Slc5a8*$^{-/-}$ (n = 19/16) animals were scored (Fig. 5, *A* and *B*). Second, colitis was induced by addition of dextran sulfate to the drinking water (23). Subsequently, animals were examined by colonoscopy. Almost all animals developed colitis, but no tumor growth was visible in WT or in *Slc5a8*$^{-/-}$ animals (n = 4/5). None of these treatments resulted in any difference in tumor growth and tumor size between WT and *Slc5a8*$^{-/-}$ animals. We also generated *Apc*^{min}/*Slc5a8*$^{-/-}$ compound mutant mice. Because the *Apc*^{min} mouse strain is known to be highly susceptible to spontaneous intestinal adenoma formation (33), we compared compound mutants to *Apc*^{min} animals (n = 11/11). Although mice carrying the *Apc*^{min} gene developed colon tumors, no significant differences between *Apc*^{min} and *Apc*^{min}/*Slc5a8*$^{-/-}$ animals became apparent (Fig. 5, *C* and *D*).

SLC5A8 Acts as a Na^+-dependent Lactate Transporter in the Colon—SLC5A8 has been described to act as an electrogenic sodium-dependent monocarboxylate and lactate transporter in heterologous expression systems such as *Xenopus* oocytes (7, 8, 10). To investigate whether SLC5A8 transports monocarboxylates in colonocytes *in vivo*, we used WT *versus Slc5a8*$^{-/-}$ colon in Ussing chamber experiments. Ion-cotransport was detected via a change of the short circuit current after donation of substrate to the luminal compartment of the colon preparation in both WT and *Slc5a8*$^{-/-}$. To analyze whether butyrate and propionate, described as having the highest affinity to SLC5A8 (7, 8), are transported by SLC5A8 at physiological concentrations (2–20 mM), both substrates were analyzed in the Ussing chamber system using colon preparations from WT and *Slc5a8*$^{-/-}$ mice. No effect was detected that could be attributed to SLC5A8-mediated transport. A similar result was obtained by determination of the flux of 5 mM sodium [^{14}C]butyrate from mucosa to serosa in WT (0.146 ± 0.016 μmol/h/cm^2) *versus* *Slc5a8*$^{-/-}$ colon (0.132 ± 0.007 μmol/h/cm^2; n = 10/9; $p >$ 0.68). These results are probably due to the dominant uptake of butyrate by SCFA/bicarbonate exchanger activity (34) and nonionic diffusion (35). Both uptake mechanisms are well described in colon although it is not clear to which proportion they contribute to colon butyrate uptake (36), because both pathways cannot be inhibited specifically.

In contrast, administration of L-lactate at the same concentration exhibited a clear change of short circuit current in WT animals (Fig. 4, *C* and *D*), which was clearly reduced in *Slc5a8*$^{-/-}$ mice (Fig. 4*C*). These findings suggest that SLC5A8 acts as a lactate transporter but not as an appreciable butyrate or propionate transporter in the colon. The addition of 2 mM Na^+-lactate to the WT colon resulted in an immediate increase of the short circuit current (Fig. 4*D*, *a* and *b*), followed by a strong decrease (Fig. 4*D*, *b* and *c*). Thereafter the current rose again until the normal value was reached after approximately 5 min. The sodium dependence of SLC5A8-mediated lactate transport was further verified in Na^+-free medium. As expected, a lactate addition at sodium-free conditions did not change the short circuit current (Fig. 4*C*). The effects demonstrated by the typical traces in Fig. 4, *C* and *D* are significant according to our calculation of the effect of lactate on the decrease of the I_{SC} following the initial increase, with this effect being markedly reduced in *Slc5a8*$^{-/-}$ (dI_{SC} = −0.29 ± 0.07 μEq/h/cm^2) *versus* WT (dI_{SC} = −0.49 ± 0.06 μEq/h/cm^2; n = 6/6; $p < 0.025$) and WT in Na^+-free medium (dI_{SC} = −0.13 ± 0.06 μEq/h/cm^2) *versus* WT (n = 5/6; $p < 0.001$).

DISCUSSION

SLC5A8 was first described as a candidate ion-cotransporter for the apical release of iodide from thyrocytes into the follicular lumen. Iodide transport by SLC5A8 was demonstrated *in vitro* by measuring the flux of $^{125}I^-$ in transfected cells (6). Subsequent studies showed that SLC5A8 acts as a monocarboxylate transporter with a variable stoichiometry of sodium:monocarboxylates in *Xenopus* oocytes, while addition of iodide did not lead to currents in the same system (7, 10). It has to be emphasized that the failure to detect a current in *Xenopus* oocytes upon iodide addition does not exclude SLC5A8 mediating fluxes of iodide in the thyroid gland. The presence and localization of SLC5A8 in the apical membrane of follicular cells clearly suggests a role for SLC5A8 in transport processes in the thyroid.

On the other hand, the loss of SLC5A8 did not impair the function of the thyroid as revealed by histology, measurement of T4 and TSH levels, and analysis of iodide organification. An obvious explanation for the lack of an overt phenotype related to iodide transport is the existence of other iodide transporters possibly compensating for SLC5A8. However, we also found that the combined inactivation of SLC5A8 and SLC26A4, both discussed as candidate cotransporters for iodide transport, did not lead to a detectable impairment of thyroid function. So far, only the inactivation of the CLC-5 chloride channel in mice might result in a delay of apical iodide efflux and goiter, although the mechanisms causing the disease are not clear (28, 37). The mutation of human *CLC-5* leads to Dent's disease not associated with thyroid dysfunction but with defects in endocytosis as demonstrated for the kidney proximal tubule (38). Therefore, it can be assumed that CLC-5 does not mediate apical iodide efflux. Altogether, none of the molecules analyzed so far seems critical for the apical release of iodide, leaving the mechanism of iodide efflux from thyrocytes open for discussion.

The physiological role of SLC5A8 clearly resides in the transport of lactate from urine and saliva as indicated by the dramatic increase in urinary loss of lactate in the *Slc5a8*$^{-/-}$ model. The expression of SLC5A8 in kidney is restricted to the apical membranes of a subset of proximal tubule cells. It has been shown earlier that SLC5A8 (SMCT1) is mainly expressed in the S3 segment of the proximal tubule, whereas the S1 and S2 segment expresses SLC5A12 (SMCT2) that may function as a low affinity transporter for monocarboxylates. In the *c/ebpδ*-null mice, besides other phenotypes (39–41), neither SLC5A8 nor SLC5A12 are expressed, and there is a urinary loss of lactate. In contrast to the model presented here, an additional urinary loss of urate is observed, and lactate concentration in the blood is reduced (12). It is not clear whether the observed differences between the *c/ebpδ* and the *Slc5a8*$^{-/-}$ are solely due to the

additional loss of *Slc5a12* or whether these changes are linked to the other physiological changes in *c/ebpδ* mice. In addition to the critical role of SLC5A8 for lactate re-absorption in kidney, we also establish a function of SLC5A8 in the adjustment of salivary lactate concentration. Given the apical expression of SLC5A8 in serous acini and ducts, we suggest that in the salivary gland SLC5A8 is required for re-absorption of lactate from the secreted saliva.

A third organ system relying on SLC5A8 for monocarboxylate transport is the intestine. Expression analysis revealed that SLC5A8 is located in the apical membrane of cells of the intestinal mucosa throughout the whole intestine, although the expression in the colon seems to be strongest. This coincides with the fact that most of the monocarboxylates produced by bacterial fermentation, such as butyrate and propionate, occur in the large intestine. Furthermore, it is reported that butyrate forms the main nutrition for the colon epithelium and is necessary for differentiation of colonocytes (42, 43). Interestingly, we found that SLC5A8 has a strong prevalence to transport lactate but does not contribute significantly to the butyrate or propionate uptake of the colon at physiological conditions. By using Ussing chambers to specifically measure SLC5A8-mediated transport of monocarboxylates in the intestine, we failed to detect a butyrate- or propionate-induced current that could be attributed to SLC5A8, yet we detected a strong induction by lactate. One has to be aware of the dominant SCFA/HCO3- exchange (34) perturbing the recordings. In addition, there is non-ionic diffusion of butyrate into the colonocytes (35). Because these components of colon butyrate transport cannot be inhibited selectively, the contribution of both components to overall colon butyrate transport is still not clear (36). These findings make the importance of SLC5A8 in transport of butyrate in the human colon (44) questionable.

Nevertheless, the strongest current was clearly detected for lactate. As expected for SLC5A8, this lactate-induced current was sodium-dependent and strongly reduced in the Slc5a8$^{-/-}$ colon. After addition of Na^+-lactate to the luminal side of the colon, we observed an immediate increase of the short circuit current due to the sodium influx mediated by SLC5A8 with a transport stoichiometry Na^+ to lactate being 2:1 (10). This increase was followed by a strong decrease. This phenomenon is well known for butyrate-induced currents and is attributed to the cell swelling following the influx of ions activating volume-dependent chloride channels responsible for the decrease (45). Thereafter, the current rose again until the normal value was reached after approximately 5 min.

SLC5A8 methylation and transcriptional down-regulation has been linked to colon cancer susceptibility or to survival rates of colon cancer patients (9, 15), and possible mechanisms for the tumor suppressive function have been suggested (32). Furthermore, there are reports on aberrant methylation of *SLC5A8* in gastric cancer and on *SLC5A8* silencing in papillary thyroid carcinomas (17) or glioma formation (18). In a thorough Affymetrix GeneChip experiment on WT *versus* *Slc5a8*$^{-/-}$ colon, we did not find any evidence of transcriptional changes caused by the lack of SLC5A8. We also examined several models of colon cancer formation in depth without any significant results regarding colon cancer susceptibility. Our results strongly question a significant impact of SLC5A8 on colon cancer susceptibility. However, we cannot rule out that other monocarboxylate transporters with a higher affinity for butyrate substitute for SLC5A8 in the mouse colon and ascertain sufficient butyrate concentrations for metabolic or other signaling events in colonocytes.

In summary, we demonstrated that SLC5A8 plays an important role in lactate re-absorption of the kidney and the salivary gland and is also involved in sodium-dependent lactate transport in the colon. The lack of an increased susceptibility for colon cancer in *Slc5a8*$^{-/-}$ mice and the failure to detect a significant uptake of butyrate by SLC5A8 argues for the dominance of other butyrate transporters, helping us to understand the physiological relevance of SLC5A8 for butyrate-mediated signaling in colonocytes.

Acknowledgments—We thank Ulrike Neckmann, Ulrike Schlapp, Diana Fuchs, and Susanne Kreutzer for excellent technical assistance. We thank Eric Green and Martin Holzenberger for providing the Pendrin- and Meu-Cre40 mouse, respectively.

REFERENCES

1. Wright, E. M., and Turk, E. (2004) *Pflugers Arch.* **447,** 510–518
2. Fraser, G. R. (1965) *Ann. Hum. Genet.* **28,** 201–249
3. Everett, L. A., Glaser, B., Beck, J. C., Idol, J. R., Buchs, A., Heyman, M., Adawi, F., Hazani, E., Nassir, E., Baxevanis, A. D., Sheffield, V. C., and Green, E. D. (1997) *Nat. Genet.* **17,** 411–422
4. Gillam, M. P., Sidhaye, A. R., Lee, E. J., Rutishauser, J., Stephan, C. W., and Kopp, P. (2004) *J. Biol. Chem.* **279,** 13004–13010
5. Everett, L. A., Belyantseva, I. A., Noben-Trauth, K., Cantos, R., Chen, A., Thakkar, S. I., Hoogstraten-Miller, S. L., Kachar, B., Wu, D. K., and Green, E. D. (2001) *Hum. Mol. Genet.* **10,** 153–161
6. Rodriguez, A. M., Perron, B., Lacroix, L., Caillou, B., Leblanc, G., Schlumberger, M., Bidart, J. M., and Pourcher, T. (2002) *J. Clin. Endocrinol. Metab.* **87,** 3500–3503
7. Coady, M. J., Chang, M. H., Charron, F. M., Plata, C., Wallendorff, B., Sah, J. F., Markowitz, S. D., Romero, M. F., and Lapointe, J. Y. (2004) *J. Physiol.* **557,** 719–731
8. Miyauchi, S., Gopal, E., Fei, Y. J., and Ganapathy, V. (2004) *J. Biol. Chem.* **279,** 13293–13296
9. Paroder, V., Spencer, S. R., Paroder, M., Arango, D., Schwartz, S., Jr., Mariadason, J. M., Augenlicht, L. H., Eskandari, S., and Carrasco, N. (2006) *Proc. Natl. Acad. Sci. U. S. A.* **103,** 7270–7275
10. Gopal, E., Fei, Y. J., Sugawara, M., Miyauchi, S., Zhuang, L., Martin, P., Smith, S. B., Prasad, P. D., and Ganapathy, V. (2004) *J. Biol. Chem.* **279,** 44522–44532
11. Barac-Nieto, M., Murer, H., and Kinne, R. (1980) *Am. J. Physiol.* **239,** F496–F506
12. Thangaraju, M., Ananth, S., Martin, P. M., Roon, P., Smith, S. B., Sterneck, E., Prasad, P. D., and Ganapathy, V. (2006) *J. Biol. Chem.* **281,** 26769–26773
13. Srinivas, S. R., Gopal, E., Zhuang, L., Itagaki, S., Martin, P. M., Fei, Y. J., Ganapathy, V., and Prasad, P. D. (2005) *Biochem. J.* **392,** 655–664
14. Gopal, E., Umapathy, N. S., Martin, P. M., Ananth, S., Gnana-Prakasam, J. P., Becker, H., Wagner, C. A., Ganapathy, V., and Prasad, P. D. (2007) *Biochim. Biophys. Acta* **1768,** 2690–2697
15. Li, H., Myeroff, L., Smiraglia, D., Romero, M. F., Pretlow, T. P., Kasturi, L., Lutterbaugh, J., Rerko, R. M., Casey, G., Issa, J. P., Willis, J., Willson, J. K., Plass, C., and Markowitz, S. D. (2003) *Proc. Natl. Acad. Sci. U. S. A.* **100,** 8412–8417
16. Ueno, M., Toyota, M., Akino, K., Suzuki, H., Kusano, M., Satoh, A., Mita, H., Sasaki, Y., Nojima, M., Yanagihara, K., Hinoda, Y., Tokino, T., and Imai, K. (2004) *Tumour Biol.* **25,** 134–140

17. Porra, V., Ferraro-Peyret, C., Durand, C., Selmi-Ruby, S., Giroud, H., Berger-Dutrieux, N., Decaussin, M., Peix, J. L., Bournaud, C., Orgiazzi, J., Borson-Chazot, F., Dante, R., and Rousset, B. (2005) *J. Clin. Endocrinol. Metab.* **90,** 3028–3035
18. Hong, C., Maunakea, A., Jun, P., Bollen, A. W., Hodgson, J. G., Goldenberg, D. D., Weiss, W. A., and Costello, J. F. (2005) *Cancer Res.* **65,** 3617–3623
19. Ganapathy, V., Gopal, E., Miyauchi, S., and Prasad, P. D. (2005) *Biochem. Soc. Trans.* **33,** 237–240
20. Leneuve, P., Colnot, S., Hamard, G., Francis, F., Niwa-Kawakita, M., Giovannini, M., and Holzenberger, M. (2003) *Nucleic Acids Res.* **31,** e21
21. Bissahoyo, A., Pearsall, R. S., Hanlon, K., Amann, V., Hicks, D., Godfrey, V. L., and Threadgill, D. W. (2005) *Toxicol. Sci.* **88,** 340–345
22. Nambiar, P. R., Girnun, G., Lillo, N. A., Guda, K., Whiteley, H. E., and Rosenberg, D. W. (2003) *Int. J. Oncol.* **22,** 145–150
23. Okayasu, I., Hatakeyama, S., Yamada, M., Ohkusa, T., Inagaki, Y., and Nakaya, R. (1990) *Gastroenterology* **98,** 694–702
24. Becker, C., Fantini, M. C., and Neurath, M. F. (2006) *Nat. Protoc.* **1,** 2900–2904
25. Irizarry, R. A., Hobbs, B., Collin, F., Beazer-Barclay, Y. D., Antonellis, K. J., Scherf, U., and Speed, T. P. (2003) *Biostatistics* **4,** 249–264
26. Benjamini, Y., and Hochberg, Y. (1995) *J. R. Statist. Soc.* **57,** 289–300
27. Westfall, P. H., and Young, S. S. (1993) *Resampling-based Multiple Testing: Examples and Methods for p-Value Adjustment*, John Wiley and Sons, New York
28. van den Hove, M. F., Croizet-Berger, K., Jouret, F., Guggino, S. E., Guggino, W. B., Devuyst, O., and Courtoy, P. J. (2006) *Endocrinology* **147,** 1287–1296
29. Harmatz, P. R., Walsh, M. K., Walker, W. A., Hanson, D. G., and Bloch, K. J. (1987) *J. Immunol. Methods* **102,** 213–219
30. Dong, S. M., Lee, E. J., Jeon, E. S., Park, C. K., and Kim, K. M. (2005) *Mod. Pathol.* **18,** 170–178
31. Schagdarsurengin, U., Gimm, O., Dralle, H., Hoang-Vu, C., and Dammann, R. (2006) *Thyroid* **16,** 633–642
32. Thangaraju, M., Gopal, E., Martin, P. M., Ananth, S., Smith, S. B., Prasad, P. D., Sterneck, E., and Ganapathy, V. (2006) *Cancer Res.* **66,** 11560–11564
33. Su, L. K., Kinzler, K. W., Vogelstein, B., Preisinger, A. C., Moser, A. R., Luongo, C., Gould, K. A., and Dove, W. F. (1992) *Science* **256,** 668–670
34. Binder, H. J., Rajendran, V., Sadasivan, V., and Geibel, J. P. (2005) *J. Clin. Gastroenterol.* **39,** S53–58
35. Charney, A. N., Micic, L., and Egnor, R. W. (1998) *Am. J. Physiol.* **274,** G518–G524
36. Chu, S., and Montrose, M. H. (1996) *J. Physiol.* **494,** 783–793
37. Maritzen, T., Lisi, S., Botta, R., Pinchera, A., Fanelli, G., Viacava, P., Marcocci, C., and Marino, M. (2006) *Thyroid* **16,** 725–730
38. Piwon, N., Gunther, W., Schwake, M., Bosl, M. R., and Jentsch, T. J. (2000) *Nature* **408,** 369–373
39. Tanaka, T., Yoshida, N., Kishimoto, T., and Akira, S. (1997) *EMBO J.* **16,** 7432–7443
40. Sterneck, E., Paylor, R., Jackson-Lewis, V., Libbey, M., Przedborski, S., Tessarollo, L., Crawley, J. N., and Johnson, P. F. (1998) *Proc. Natl. Acad. Sci. U. S. A.* **95,** 10908–10913
41. Thangaraju, M., Rudelius, M., Bierie, B., Raffeld, M., Sharan, S., Hennighausen, L., Huang, A. M., and Sterneck, E. (2005) *Development* **132,** 4675–4685
42. Roy, C. C., Kien, C. L., Bouthillier, L., and Levy, E. (2006) *Nutr. Clin. Pract.* **21,** 351–366
43. Wong, J. M., de Souza, R., Kendall, C. W., Emam, A., and Jenkins, D. J. (2006) *J. Clin. Gastroenterol.* **40,** 235–243
44. Dohgen, M., Hayahshi, H., Yajima, T., and Suzuki, Y. (1994) *Jpn. J. Physiol.* **44,** 519–531
45. Diener, M., Peter, A., and Scharrer, E. (1994) *Acta Physiol. Scand.* **151,** 385–394